Expert Systems with Applications 38 (2011) 7334–7341

Contents lists available at ScienceDirect

Expert Systems with Applications

journal homepage: www.elsevier.com/locate/eswa

EEMD method and WNN for fault diagnosis of locomotive roller bearings

Yaguo Lei *, Zhengjia He, Yanyang Zi

State Key Laboratory for Manufacturing Systems Engineering, Xi'an Jiaotong University, Xi'an 710049, PR China

ARTICLE INFO

Keywords:
Ensemble empirical mode decomposition
Intrinsic mode function
Wavelet neural network
Bearing fault diagnosis

ABSTRACT

The ensemble empirical mode decomposition (EEMD) can overcome the mode mixing problem of the empirical mode decomposition (EMD) and therefore provide more precise decomposition results. Wavelet neural network (WNN) possesses the advantages of both wavelet transform and artificial neural networks. This paper combines the merits of EEMD and WNN to propose an automated and effective fault diagnosis method of locomotive roller bearings. First, the vibration signals captured from the locomotive roller bearings are preprocessed by EEMD method and intrinsic mode functions (IMFs) are produced. Second, a kurtosis based method is presented and used to select the sensitive IMF. Third, time- and frequency-domain features are extracted from the sensitive IMF, its frequency spectrum and its envelope spectrum. Finally, these features are fed into WNN to identify the bearing health conditions. The diagnosis results show that the proposed method enables the identification of the single faults in the bearings and at the same time the recognition of the fault severities and the compound faults.

1. Introduction

Roller bearings are at the heart of rotating machinery. In rotating machinery, the failure of roller bearings can result in the deterioration of machine operating conditions. Therefore, it is significant to be able to accurately and automatically detect and diagnose the existence and severity of the faults occurring in the bearings (Lei, He, & Zi, 2008). Because vibration signals carry a great deal of information representing mechanical equipment health conditions, the vibration based signal processing technique is one of the principal tools for diagnosing bearing faults (Lei, He, Zi, & Hu, 2008; Zarei & Poshtan, 2009). With the signal processing techniques, fault characteristic information can be extracted from the vibration signals.

Empirical mode decomposition (EMD) is a new signal processing technique. It is based on the local characteristic time scales of a signal and could decompose the complicated signal into intrinsic mode functions (IMFs) (Huang, Shen, & Long, 1998). The IMFs represent the natural oscillatory mode embedded in the signal and work as the basis functions, which are determined by the signal itself. Thus, it is a self-adaptive signal processing method and has been widely applied in fault diagnosis of roller bearings recently (Cheng, Yu, & Yang, 2007; Lei, He, & Zi, 2007; Rai & Mohanty, 2007). However, one of the major drawbacks of EMD is the mode mixing problem, which is defined as either a single IMF consisting of components of widely disparate scales, or a component of a similar scale residing in different IMFs. To alleviate the problem of mode mixing in EMD, ensemble empirical mode decomposition (EEMD) was presented recently (Wu & Huang, 2009). EEMD is a noise-assisted data analysis method and by adding finite white noise to the investigated signal, the EEMD method can eliminate the mode mixing problem automatically. Therefore, the EEMD represents a major improvement of EMD. The application of the EEMD to rotor fault diagnosis has demonstrated the effectiveness of the EEMD method in fault diagnosis of rotating machinery (Lei, He, & Zi, 2008).

However, fault diagnosis methods only using advanced signal processing techniques require a good deal of expertise to apply them successfully. Simpler methods are needed which allow relatively unskilled operators to make reliable decisions without the need for a diagnosis specialist to examine data and diagnose problems. Therefore, there is a demand for techniques that can make decision on the running health of the machine automatically (Lei, He, Zi, et al., 2008; Wong, Jack, & Nandi, 2006). Artificial neural networks, such as multi-layer perceptron (MLP) neural network, and radial basis function (RBF) neural network have been successfully applied to automated machine fault diagnosis and increased the accuracy of fault detection and diagnosis systems (Lei, He, & Zi, 2008; Samanta, 2004; Wu & Liu, 2008). Wavelet neural network (WNN) is developed as an alternative to feed forward neural networks based on wavelet transform theory. It combines the characteristics of time–frequency location of the wavelet transform and self-learning capability of artificial neural networks (Zhang & Benveniste, 1992). Therefore, WNN simultaneously possesses the advantages of wavelet transform and artificial neural networks.

* Corresponding author.
E-mail address: leiyaguo@gmail.com (Y. Lei).

0957-4174/$ - see front matter © 2010 Elsevier Ltd. All rights reserved.
doi:10.1016/j.eswa.2010.12.095

To automatically and effectively diagnose faults of locomotive roller bearings, a fault diagnosis method based on EEMD and WNN is proposed in this paper. In the proposed method, the vibration signals captured from the bearings are first decomposed by the EEMD method. Second, the most sensitive IMF is selected. Third, time- and frequency-domain features are extracted from the most sensitive IMF, its frequency spectrum and Hilbert envelope spectrum. Finally, these features are input into WNN to recognize the health conditions of the locomotive roller bearings. The vibration signals are measured from the locomotive roller bearings under the different health conditions including the different fault categories, fault severities and compound faults. The identification result validates the effectiveness of the proposed method.

2. Experimental setup and data acquisition

The test bench of a locomotive roller bearing is shown in Fig. 1. The test bench consists of a hydraulic motor, two supporting pillow blocks (mounting with normal bearing), a tested bearing (52732QT) which is loaded on the outer race by a hydraulic cylinder, a hydraulic radial load application system, and a tachometer for shaft speed measurement. The bearing is installed in a hydraulic motor driven mechanical system. 608A11-type ICP accelerometers are mounted on the load module adjacent to the outer race of the tested bearing for measuring its vibrations. The advanced data acquisition and analysis system by Sony EX is used to collect the data. Some parameters in the experiment are listed in Table 1.

A bearing data set containing nine subsets is obtained from the experimental system under the nine different health conditions. The nine conditions are described in Table 2. In the nine bearing conditions, serious fault in the outer race (condition 2) is serious flaking fault, and the other faults are all slight rub. These faulty bearings are shown in Fig. 2. Each data subset corresponds to one of the nine conditions and it consists of 50 samples. Each sample is a vibration signal containing 8192 sampling points. Fig. 3(a)–(i) give raw data samples for the nine bearing health conditions: (a) normal condition, (b) slight rub fault in the outer race, (c) serious flaking fault in the outer race, (d) slight rub fault in the inner race, (e) roller rub fault, (f) compound faults in the outer and inner races, (g) compound faults in the outer race and roller, (h) compound faults in the inner race and roller, and (i) compound faults in the outer and inner races and roller.

3. Empirical mode decomposition and ensemble empirical mode decomposition

3.1. EMD algorithm and mode mixing

The EMD method is able to decompose the complicated signal into a set of complete and almost orthogonal components IMFs. An IMF is the function that satisfies the two following conditions:

Table 1
Parameters in the experiment.

Parameter	Value
Bearing specs	552732QT
Load	9800 N
Inner race diameter	160 mm
Outer race diameter	290 mm
Roller diameter	34 mm
Roller number	17
Contact angle	0°
Sampling frequency	12.8 kHz

Table 2
Description of the faulty bearings.

Condition	Rotating speed (rpm)	Label
(a) Normal condition	About 490	1
(b) Slight rub fault in the outer race	About 490	2
(c) Serious flaking fault in the outer race	About 480	3
(d) Slight rub fault in the inner race	About 500	4
(e) Roller rub fault	About 530	5
(f) Compound faults in the outer and inner races	About 520	6
(g) Compound faults in the outer race and rollers	About 520	7
(h) Compound faults in the inner race and rollers	About 640	8
(i) Compound faults in the outer and inner races and rollers	About 550	9

Fig. 2. Faults in the locomotive roller bearings.

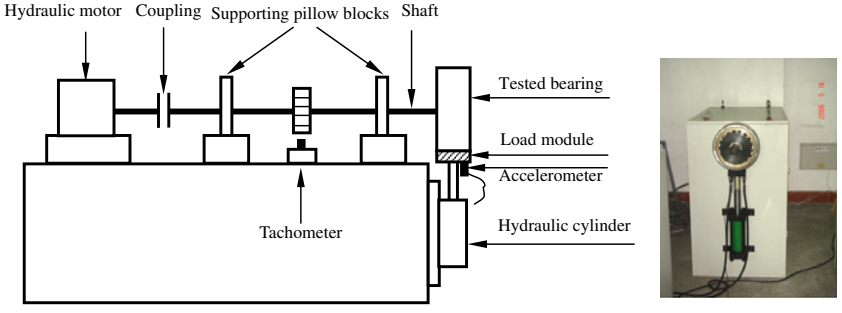

Fig. 1. Test bench of the locomotive roller bearing.

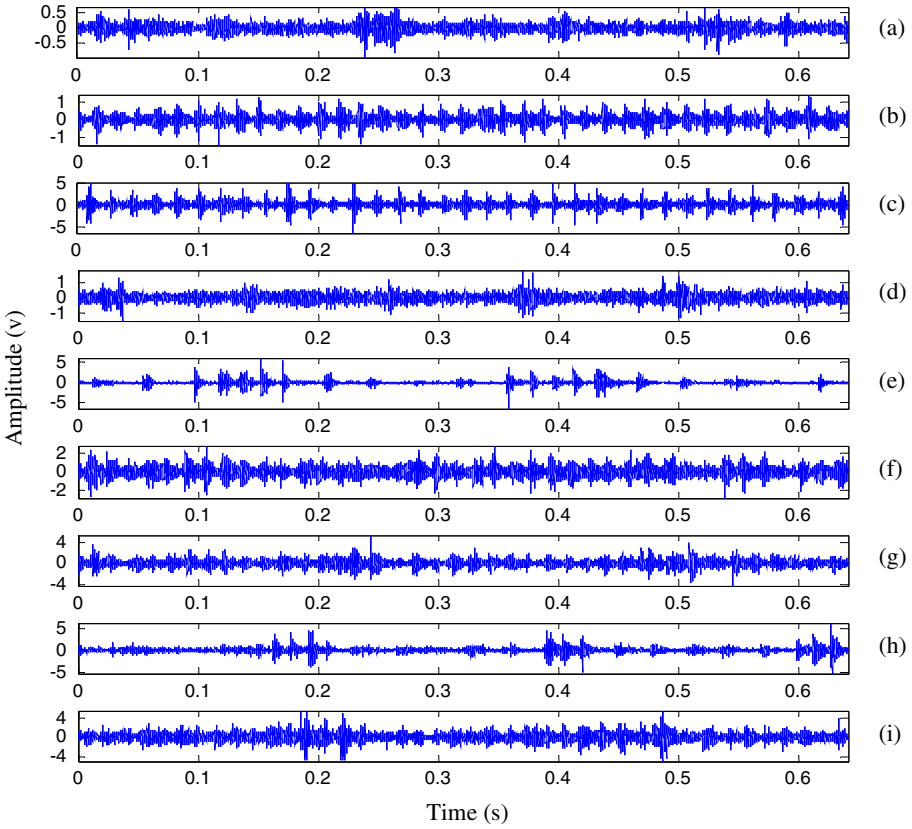

Fig. 3. Data samples of the nine bearing conditions.

(1) in the whole data set, the number of extrema and the number of zero-crossings must either equal or differ at most by one, and (2) at any point, the mean value of the envelope defined by local maxima and the envelope defined by the local minima is zero (Huang et al., 1998). An IMF represents simple oscillatory mode embedded in the signal. With the simple assumption that any signal consists of different simple IMFs, the EMD method was developed to decompose a signal into IMF components. The EMD process can be found in Huang et al. (1998).

However, the EMD method has a shortcoming, which is the mode mixing problem. Mode mixing is defined as a single IMF including oscillations of dramatically disparate scales, or a component of a similar scale residing in different IMFs. It is a result of signal intermittency. As discussed by Huang et al. (1998), the intermittence could not only cause serious aliasing in the time–frequency distribution, but also make physical meaning of individual IMF unclear. When the mode mixing problem occurs, an IMF can cease to have physical meaning by itself, suggesting falsely that there may be different physical processes represented in a mode.

To illustrate the mode mixing problem in EMD, a simulation signal $x(t)$ is considered in this section. The simulation signal, shown in Fig. 4(a), is a sine wave of 36 Hz attached by small impulses. Thus, it is a combined signal and involves two components. Performing EMD on the signal, the decomposed two IMFs are shown in Fig. 4(b) and (c).

It is obvious that the two IMFs obtained by EMD are distorted seriously. Mode mixing is occurring between IMFs c_1 and c_2. The sine wave and the impulses are decomposed into the same IMF (c_1). Moreover, the sine wave is decomposed into two IMFs. Thus, both IMFs c_1 and c_2 of EMD fail to reflect the characteristics of signal $x(t)$ accurately. This is a typical problem of mode mixing.

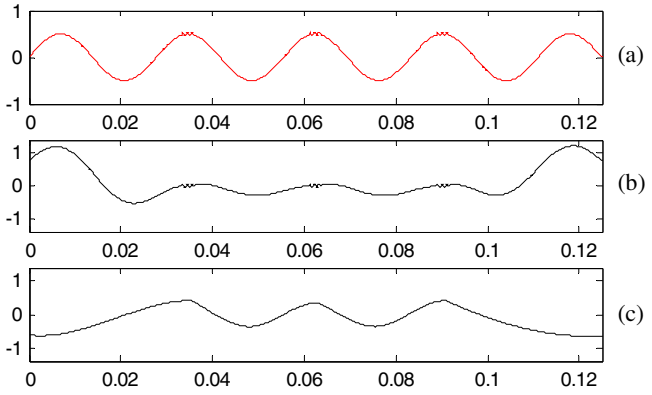

Fig. 4. The decomposition result with EMD: (a) the simulation signal, (b) IMF c_1, and (c) IMF c_2.

3.2. Ensemble empirical mode decomposition

To solve the problem of mode mixing in EMD, ensemble empirical mode decomposition (EEMD) was proposed, which defines the true IMF components as the mean of an ensemble of trials (Wu & Huang, 2009). Each trial consists of the decomposition results of the signal plus a white noise of finite amplitude. This new method is based on the insight from recent studies of the statistical properties of white noise (Flandrin, Rilling, & Gonçalvès, 2004; Wu & Huang, 2004), which showed that the EMD method is an effective self-adaptive dyadic filter bank when applied to the white noise. Additionally, the result studied by Flandrin et al. (2005) demonstrated that noise could help data analysis in the EMD method. All these investigation promotes the advent of the EEMD method.

The principle of the EEMD algorithm is the following: the added white noise would populate the whole time–frequency space uniformly with the constituting components of different scales. When a signal is added to this uniformly distributed white noise background, the components in different scales of the signal are automatically projected onto proper scales of reference established by the white noise in the background. Because each of the noise-added decompositions consists of the signal and the added white noise, each individual trial may certainly produce very noisy results. But the noise in each trial is different in separate trials. Thus it can be decreased or even completely canceled out in the ensemble mean of enough trails. The ensemble mean is treated as the true answer because the only persistent part is the signal as more and more trials are added in the ensemble.

The EEMD algorithm can be given as follows.

(1) Initialize the number of ensemble M, the amplitude of the added white noise, and $m = 1$.
(2) Perform the mth trial on the signal added white noise.
  (a) Add a white noise series with the given amplitude to the investigated signal.

$$X_m(t) = x(t) + n_m(t), \tag{1}$$

  where $n_m(t)$ indcates the mth added white noise series, and $x_m(t)$ represents the noise-added signal of the mth trial.
  (b) Decompose the noise-added signal $x_m(t)$ into I IMFs $c_{i,m}$ ($i = 1, 2, \ldots, I$) using the EMD method, where $c_{i,m}$ denotes the ith IMF of the mth trial, and I is the number of IMFs.
  (c) If $m < M$ then go to step (a) with $m = m + 1$. Repeat steps (a) and (b) again and again, but with different white noise series each time.
(3) Calculate the ensemble mean a_i of the M trials for each IMF

$$a_i = \frac{1}{M}\sum_{m=1}^{m} c_{i,m}, \quad i = 1, 2, \ldots, I, \ m = 1, 2, \ldots, M. \tag{2}$$

(4) Report the mean ai ($i = 1, 2, \ldots, I$) of each of the I IMFs as the final IMFs.

To demonstrate the EEMD performance of overcoming the mode mixing problem, the simulation signal in Fig. 4(a) is decomposed again using EEMD with the ensemble number 100 and the added noise amplitude 0.01 time standard deviation of the signal. The decomposition result is shown in Fig. 5. From Fig. 5(b) and (c), it is seen that the two components included in the signal are decomposed into two IMFs perfectly. IMF a_1 denotes the impulse components and IMF a_2 indicates the sine wave. Thus, the EEMD method is able to solve the problem of mode mixing and achieve an improved decomposition with physical meaning.

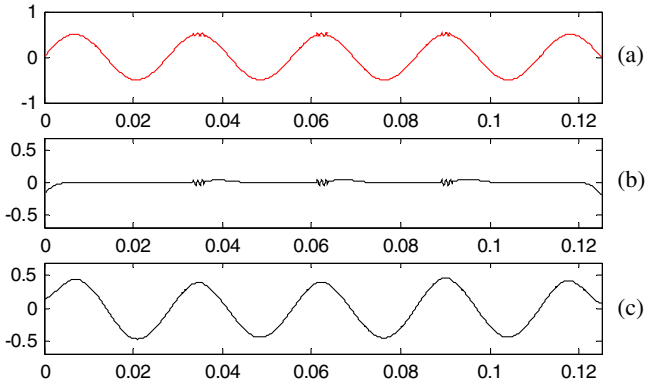

Fig. 5. The decomposition result with EEMD: (a) the simulation signal, (b) IMF a_1, and (c) IMF a_2.

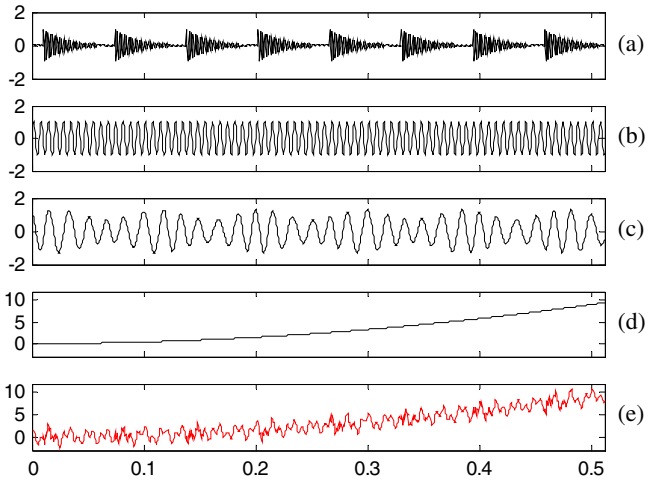

Fig. 6. The four components and the simulation signal: (a)–(d) the four components, (e) the simulation signal.

3.3. Simulation experiment

Modulation and impact are two typical fault events in machine fault diagnosis. Therefore, the EEMD method is tested on a simulation signal including modulation and impact components. The simulation signal also consists of a sine wave representing a certain rotating frequency of machinery and a trend item (Lei et al., 2008). Thus, there are altogether four components corresponding to different physical meanings in the simulation signal. The four components and the simulation signal produced by combining the four components are shown in Fig. 6(a)–(e), respectively.

Applying the EEMD method to the decomposition of the simulation signal, the decomposition result is given in Fig. 7. It can be seen from Fig. 7 that components a_1, a_2, a_3 and a_4, respectively correspond to the impact component, the certain rotating frequency, the modulation component and the trend item. Comparing the decomposed components shown in Fig. 7 with the real components given in Fig. 6, it is found that the different components embedded in the signal can be extracted accurately using the EEMD method.

For comparison, the simulation signal is analyzed again using the EMD method and the decomposition result is displayed in

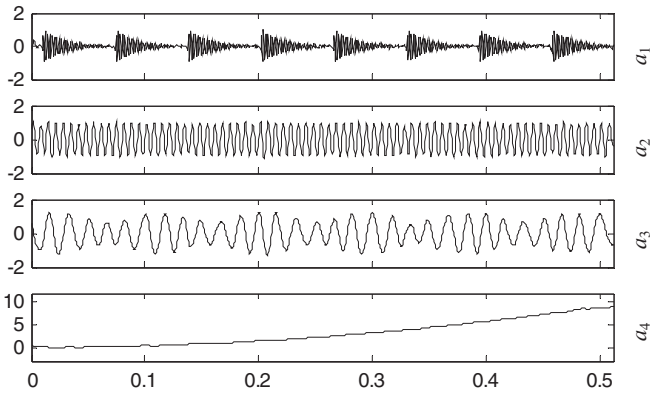

Fig. 7. The decomposed four components with EEMD.

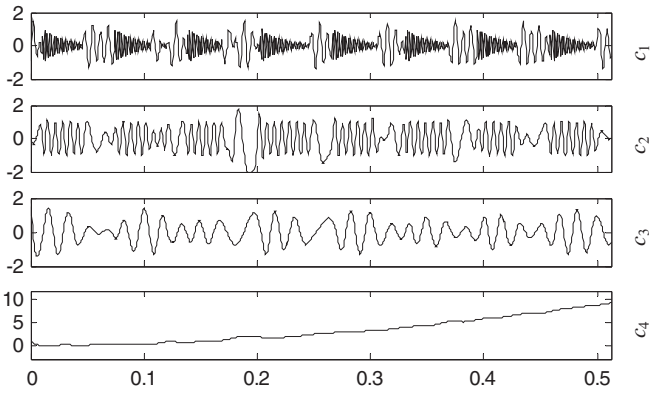

Fig. 8. The decomposed four components with EMD.

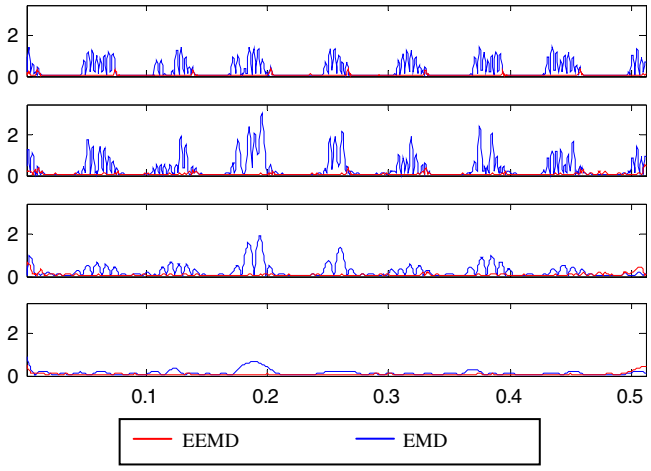

Fig. 9. The decomposition errors of EEMD and EMD.

Fig. 8. It is clear that the problem of mode mixing appears between different IMFs and there are serious distortions for each IMF. This result shows that the EMD method fails to provide the reasonable decomposition. Additionally, observing the errors of EEMD and EMD shown in Fig. 9, which are obtained through calculating the absolute values of the differences between the decomposition components and the corresponding real components as shown in Fig. 6, the errors of EEMD are far smaller than those of EMD. Thus, the decomposition result of the EEMD method is better than that of the EMD method.

4. Sensitive IMF selection and feature extraction

4.1. Sensitive IMF selection

According to the above comparison between EMD and EEMD, it can be seen that EEMD not only inherits the advantages of EMD in decomposing nonlinear and non-stationary signals but also overcomes the problem of mode mixing of EMD. In order to extract bearing fault-related component and avoid interference of other components, the EEMD method is used to decompose the vibration signals of the locomotive roller bearings. Generally, one more IMFs will be obtained and we can select the sensitive IMF to further process.

When local defects, such as rub and flaking, occurs in the outer race, inner race and roller of bearings, the vibration signals captured from the bearings show a series of impulses. Kurtosis is widely used to detect impulse components caused by local defects (Qu & He, 1986). Here, a method based on kurtosis is presented to select the sensitive IMF from all IMFs generated by EEMD.

(1) For each of the nine bearing health conditions in this paper, the kurtosis values of I IMFs of each of the data samples are calculated. Let $k_{i,s}$ denote the kurtosis of the ith IMF of the sth data sample and it is expressed as:

$$k_{i,s} = \frac{N\sum_{n=1}^{N}(a_{n,i} - \overline{a_i})^4}{N\sum_{n=1}^{N}(a_{n,i} - \overline{a_i})^2)}, \quad n = 1,2,\ldots,N, \\ i = 1,2,\ldots,I, \ s = 1,2,\ldots,S, \tag{3}$$

where $a_{n,i}$ is the nth measurement in the ith IMF a_i, $\overline{a_i}$ is the average of a_i, N is the number of data points of IMF a_i, I is the number of IMFs, and S is the number of data samples.

(2) Calculate the mean and standard deviation of kurtosis values of S data samples for each IMF

$$m_i = \frac{1}{S}\sum_{s=1}^{S} k_{i,s} \quad i = 1,2,\ldots,I, \tag{4}$$

where m_i is the mean of kurtosis values of the ith IMF of S data samples.

$$std_i = \sqrt{\frac{1}{(S-1)}\sum_{s=1}^{S}(k_{i,s} - m_i)^2}, \quad i = 1,2,\ldots,I, \tag{5}$$

where std_i is the standard deviation of kurtosis values of the ith IMF of S data samples.

(3) Construct the criterion of the sensitive IMF selection. For the normal bearings, the kurtosis value of each IMF is small. But when the bearings have local defects, the kurtosis value will increase. Thus, normal bearings have smaller mean m_i of IMF kurtosis values than faulty bearings. In addition, whether the bearing health condition is normal or faulty, smaller standard deviation std_i of kurtosis values of each IMF is easier to distinguish different bearing conditions. Therefore, we construct the following selection criterion of the sensitive IMF.

$$f_i = \begin{cases} m_i \cdot std_i, & \text{for normal bearings} \\ \frac{std_i}{m_i}, & \text{for faulty bearings} \end{cases} i = 1,2,\ldots,I. \tag{6}$$

(4) Select the sensitive IMF under each of the nine bearing health conditions. According to the definition of the selection criterion, the IMF making Eq. (6) smallest is the sensitive IMF. For the nine bearing health conditions in this study, the most frequently selected IMF is IMF a_1. Thus, a_1 is the sensitive IMF and will be further processed to extract features.

4.2. Feature extraction

For fault diagnosis of the locomotive roller bearings in this paper, both time- and frequency-domain features are extracted to recognize various bearing health conditions. They are standard deviation (x_{std}), kurtosis (x_{kur}), shape factor (SF) and impulse factor (IF) in the time domain, and mean frequency (x_{mf}), root mean square frequency (x_{msf}), standard deviation frequency (x_{stdf}) and spectrum peak ratio of bearing outer race ($SPRO$), inner race ($SPRI$) and roller ($SPRR$) in the frequency domain.

First, four time-domain features are extracted from IMF a_1 of each of the collected vibration signals. Then three frequency-domain features x_{mf}, x_{msf} and x_{stdf} are extracted from the frequency spectrum of IMF a_1.

Table 3
The extracted 10 features.

1	Standard deviation	x_{std}	6	Root mean square frequency	x_{rmsf}
2	Kurtosis	x_{kur}	7	Standard deviation frequency	x_{stdf}
3	Shape factor	SF	8	Spectrum peak ratio of bearing outer race	$SPRO$
4	Impulse factor	IF	9	Spectrum peak ratio of bearing inner race	$SPRI$
5	Mean frequency	x_{mf}	10	Spectrum peak ratio of bearing roller	$SPRR$

Demodulation detection makes the diagnosis process a little more independent of a particular machine since it focuses on the low-amplitude high-frequency broadband signals reflecting machine conditions (Benko, Petrovčič, Juričić, Tavčar, & Rejec, 2005). Defining a signal $x(t)$, we can have its Hilbert transform as follows:

$$H[x(t)] = \frac{\int_{-\infty}^{\infty} \frac{x(t)}{t-\tau} d\tau}{\pi}. \quad (7)$$

Then the Hilbert envelope spectrum can be given as follows:

$$h(f) = \int_{-\infty}^{\infty} \sqrt{x^2(t) + H^2[x(t)]} e^{-j2\pi ft} dt. \quad (8)$$

For IMF a_1, we perform the Hilbert transform on it and calculate its envelope spectrum. Then additional three frequency-domain features *SPRO*, *SPRI* and *SPRR* are extracted from the envelope spectrum of IMF a_1. Therefore, 10 features are produced from IMF a_1 of each vibration signal, the frequency spectrum and the envelope spectrum of IMF a_1. These 10 features are shown in Table 3. They will be input into a subsequent classifier to automatically identify the health conditions of the locomotive roller bearings.

5. The proposed bearing fault diagnosis method

5.1. Brief review of WNN

WNN is proposed as an alternative to feed forward neural networks for approximating arbitrary nonlinear functions based on the wavelet transform theory (Zhang & Benveniste, 1992). In WNN, wavelet basis functions are used as node activation functions. WNN introduces the wavelet decomposition property into a general neural network, and combines the advantage of time–frequency location of the wavelet transform and self-learning capability of artificial neural networks. Thus, it possesses doughty capability of approximate and robust.

The WNN in this paper is designed as a three-layer structure with an input layer, a hidden layer, and an output layer. Each layer has one or more nodes. Fig. 10 shows the schematic diagram of the three-layer WNN and I_n^k is the nth input feature of the kth data sample. Morlet wavelet is widely used as the activation function in the nodes of the hidden layer (Ghohizadeh, Salajegheh, & Torkzadeh, 2008; Subasi, Alkan, Koklukaya, & Kiymika, 2005). It is expressed by Eq. (9) and shown in Fig. 11.

$$W(t) = \cos(4t) \exp\left(-\frac{t^2}{2}\right). \quad (9)$$

The training of WNN involves optimizing both the position and dilation of the wavelets besides the weights, which minimize an error function between the actual network outputs and the corresponding target outputs in the training samples. The back propagation algorithm is commonly adopted for the training of WNN in the literature (Chen, Yang, & Dong, 2006; Lin, Shen, & Kung, 2005) and it is also employed in the designed WNN of this paper.

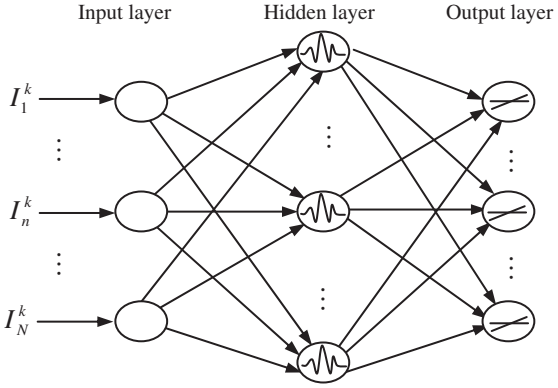

Fig. 10. Schematic diagram of the three-layer WNN.

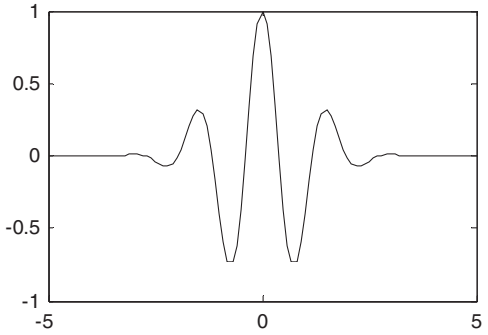

Fig. 11. Morlet wavelet activation function.

5.2. The proposed diagnosis method

The proposed bearing fault diagnosis method based on EEMD and WNN is shown in Fig. 12. It includes the following four procedures. First, each of the vibration signals collected from the locomotive roller bearings is decomposed into a set of IMFs with EEMD. Second, the sensitive IMF is selected from all IMFs via a kurtosis based method presented in this paper. Third, 10 features including time- and frequency-domain features are extracted from the selected sensitive IMF, its frequency spectrum and its Hilbert envelope spectrum. Finally, WNN is applied to the health condition identification of the locomotive roller bearings and final diagnosis result can be produced.

6. Fault diagnosis of the locomotive roller bearings

6.1. Experiments and results

In this section, three experiments over three different data sets selected from the whole data set of locomotive roller bearings, are conducted to demonstrate the effectiveness of the proposed method. For comparison, MLP neural network with three layers and RBF neural network are also employed to analyze the same data sets, respectively. MLP neural network, RBF neural network and WNN have the same node number of input layer, hidden layer and output layer in this paper. They are 10, 12 and 1, respectively.

6.1.1. Experiment 1: diagnosis performance comparison of different fault categories

In this experiment, a bearing data set consisting of the four data subsets acquired respectively under normal condition, serious fault in the outer race, inner race fault and roller fault, is applied to

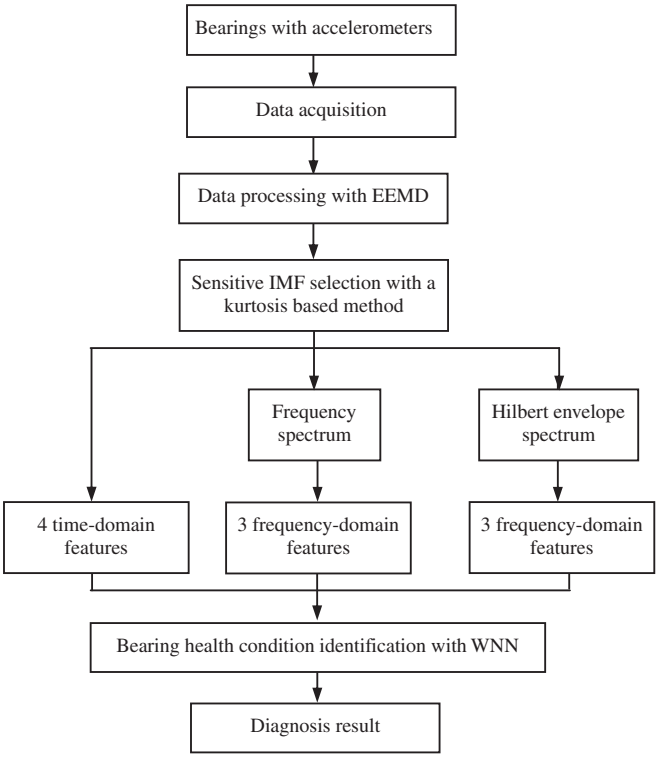

Fig. 12. Flow chart of the proposed method.

evaluate the performance of the proposed method in recognizing different fault categories of the locomotive roller bearings. As mentioned in Section 2, each of the four data subsets contains 50 samples, and therefore the whole data set corresponding to the four bearing health conditions includes altogether 200 samples. The whole data set is split into two sets: 100 samples for training and 100 for testing.

Using the 10 features extracted in Section 4.2 as the input features, the three classifiers based on MLP neural network, RBF neural network and WNN are respectively trained and tested to identify the fault categories of the locomotive roller bearings. The testing results are shown in Table 4 and Fig. 13, respectively. For this experiment, MLP neural network, RBF neural network and WNN produce the classification accuracies of 89%, 90% and 100%, respectively. The proposed method based on WNN achieves the best identification result. It improves the diagnosis accuracy by 11% and 10%, respectively compared with MLP and RBF. This comparison result implies that the proposed method obviously outperforms the other two methods in diagnosing different categories of bearing faults.

6.1.2. Experiment 2: diagnosis performance comparison of different fault severities

To examine the effect of the proposed method in identifying different fault severities, the proposed method is performed on a data set containing different fault severities. The data set has 150 samples: 50 samples being normal condition, 50 samples for slight fault in the outer race and the rest 50 belonging to serious fault in the outer race. 75 samples of the 150 samples form the training set and the remaining 75 samples are the testing set.

Table 4
Testing accuracies of MLP neural network, RBF neural network and WNN in the three experiments (%).

Experiment	MLP	RBF	WNN
1	89	90	100
2	100	100	100
3	67.56	78.67	91.56

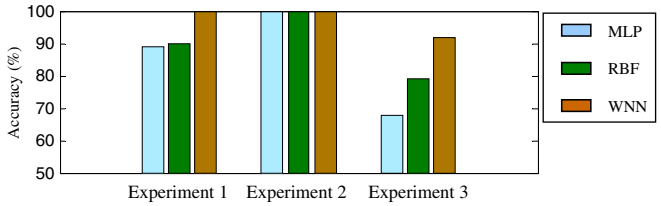

Fig. 13. Testing accuracies of the three neural networks in the three experiments.

The testing results of the three neural networks on the identification of the different fault severities are listed in Table 4 and shown in Fig. 13, respectively. Since this experiment is a three-class classification problem and relatively simple, all the neural networks obtain the high testing accuracy (100%).

6.1.3. Experiment 3: diagnosis performance comparison of compound faults

Besides the different categories of a single fault and the different fault severities, compound faults generally also occur in roller bearings. If they can not be detected as early as possible, they will usually lead to a more serious consequence. Thus, it is of considerable practical value to diagnose the compound faults in bearings correctly and in time.

In this experiment, a data set containing not only the different fault categories and severities but also the compound faults is analyzed. The data set represents the nine conditions (described in Table 2) of the locomotive roller bearings and consists of 450 samples. The 450 data samples are divided into 225 training and 225 testing instances.

Table 4 and Fig. 13 present the testing results of MLP neural network, RBF neural network and WNN in this experiment. From the table and the figure, it can be seen that the testing accuracies of the three methods are respectively 67.56%, 78.67% and 91.56%. The diagnosis accuracies of this experiment decrease because this is a ten-class classification problem and therefore relatively difficult. But the highest testing accuracy is still achieved by the proposed method. These imply that the proposed method can identify not only the different fault categories and severities but also the compound faults better.

6.2. Discussion

(1) The diagnosis results in the above experiments prove that the proposed method based on EEMD and WNN obtains obvious improvement in recognition accuracy and provides a good diagnosis capability. It reliably recognizes not only the different fault categories and severities but also the compound faults. The reasons are as follows. (1) Preprocessing with EEMD overcomes the mode mixing problem of EMD and increases the decomposition precision of vibration signals. (2) Selecting the sensitive IMF reflecting the bearing fault characteristics avoids interference of other fault-unrelated components. (3) Extracting features from both time and frequency domains better represents the health conditions of the locomotive roller bearings. (4) Adopting the classifier based on WNN raises diagnosis accuracy.

(2) The EEMD method is able to solve the problem of mode mixing existing in the EMD method and achieve better decomposition results than EMD. Thus, the EEMD method is a powerful tool for nonlinear and non-stationary signal

analysis. However, the EEMD method introduces its own problems that have to do with the magnitude of noise and number of ensembles. Generally, aiming at the specific diagnosis problem, different noise magnitudes and ensemble numbers need to be tried and selected. The authors would like to investigate this research topic in future.

(3) WNN is a promising tool to pattern recognition problems. In this paper, we use it to classify the different fault categories, different severities and compound faults. Although it has produced the satisfactory results in identifying health conditions of the locomotive roller bearings, the network initialization, the optimum structure selection and the training algorithm are issues affecting the performance of WNN. These issues will be investigated in our future work.

(4) The problems studied in this paper cover single fault diagnosis, slight fault diagnosis and compound fault diagnosis, and therefore they are typical cases of roller bearing fault diagnosis. The satisfactory experiment results demonstrate the effectiveness and generalization ability of the proposed method.

7. Conclusions

Based on ensemble empirical mode decomposition (EEMD) and wavelet neural network (WNN), this paper presents an automated and effective fault diagnosis method of locomotive roller bearings. In the presented method, the EEMD method is performed to preprocess bearing vibration signals. With a kurtosis based method presented in this paper, the sensitive intrinsic mode function (IMF) is selected from all IMFs produced by EEMD. Then, 10 time- and frequency-domain features are extracted from the sensitive IMF and fed into WNN to identify the bearing health conditions. The diagnosis results demonstrate that the proposed method can reliably recognize not only the single faults and the different fault severities but also the compound faults.

Acknowledgements

This work was supported by National Science Foundation of China (51005172), the Fundamental Research Funds for the Central Universities and the Preferred Support Funds of the Scientific Research Project of the Ministry of Human Resources and Social Security of China for Returned Scholars.

References

Benko, U., Petrovčič, J., Juričić, D., Tavčar, J., & Rejec, J. (2005). An approach to fault diagnosis of vacuum cleaner motors based on sound analysis. *Mechanical Systems and Signal Processing, 19*, 427–445.

Chen, Y., Yang, B., & Dong, J. (2006). Time-series prediction using a local linear wavelet neural network. *Neurocomputing, 69*, 449–465.

Cheng, J. S., Yu, D. J., & Yang, Y. (2007). The application of energy operator demodulation approach based on EMD in machinery fault diagnosis. *Mechanical Systems and Signal Processing, 21*, 668–677.

Flandrin, P., Gonçalvès, P., & Rilling, G. (2005). EMD equivalent filter banks, from interpretation to applications. In N.E. Huang & S.S.P. Shen (Eds.), *Hilbert–Huang transform: Introduction and applications* (pp. 67–87, 360pp.). Singapore: World Scientific.

Flandrin, P., Rilling, G., & Gonçalvès, P. (2004). Empirical mode decomposition as a filter bank. *IEEE Signal Processing Letter, 11*, 112–114.

Ghohizadeh, S., Salajegheh, E., & Torkzadeh, P. (2008). Structural optimization with frequency constraints by genetic algorithm using wavelet radial basis function neural network. *Journal of Sound and Vibration, 312*, 316–331.

Huang, N. E., Shen, Z., & Long, S. R. (1998). The empirical mode decomposition and the Hilbert spectrum for nonlinear and non-stationary time series analysis. *Proceedings of the Royal Society of London, 454*, 903–995.

Lei, Y. G., He, Z. J., & Zi, Y. Y. (2007). Fault diagnosis of rotating machinery based on multiple ANFIS combination with GAs. *Mechanical Systems and Signal Processing, 21*, 2280–2294.

Lei, Y. G., He, Z. J., & Zi, Y. Y. (2008). Application of a novel hybrid intelligent method to fault diagnosis of locomotive roller bearings. *Transactions of the ASME: Journal of Vibration and Acoustics, 130*, 0345011–0345016.

Lei, Y. G., He, Z. J., Zi, Y. Y., & Hu, Q. (2008). Fault diagnosis of rotating machinery based on a new hybrid clustering algorithm. *International Journal of Advanced Manufacturing Technology, 35*, 968–977.

Lei, Y. G., He, Z. J., & Zi, Y. Y. (2008). A new approach to intelligent fault diagnosis of rotating machinery. *Expert Systems with Applications, 35*, 1593–1600.

Lei, Y. G., He, Z. J., Zi, Y. Y., et al. (2008). New clustering algorithm-based fault diagnosis using compensation distance evaluation technique. *Mechanical Systems and Signal Processing, 22*, 419–435.

Lei, Y. G., He, Z. J., & Zi, Y. Y. (2008). Application of the EEMD method to rotor fault diagnosis of rotating machinery. *Mechanical Systems and Signal Processing*. doi:10.1016/j.ymssp.2008.11.005.

Lin, F. J., Shen, P. H., & Kung, Y. S. (2005). Adaptive wavelet neural network control for linear synchronous motor servo drive. *IEEE Transactions on Magnetics, 41*, 4401–4412.

Qu, L., & He, Z. (1986). *Mechanical diagnostics*. PR China: Shanghai Science and Technology Press.

Rai, V. K., & Mohanty, A. R. (2007). Bearing fault diagnosis using FFT of intrinsic mode functions in Hilbert–Huang transform. *Mechanical Systems and Signal Processing, 21*, 2607–2615.

Samanta, B. (2004). Gear fault detection using artificial neural networks and support vector machines with genetic algorithms. *Mechanical Systems and Signal Processing, 18*, 625–644.

Subasi, A., Alkan, A., Koklukaya, E., & Kiymika, M. K. (2005). Wavelet neural network classification of EEG signals by using AR model with MLE preprocessing. *Neural Networks, 18*, 985–997.

Wong, M. L. D., Jack, L. B., & Nandi, A. K. (2006). Modified self-organising map for automated novelty detection applied to vibration signal monitoring. *Mechanical Systems and Signal Processing, 20*, 593–610.

Wu, Z. H., & Huang, N. E. (2004). A study of the characteristics of white noise using the empirical mode decomposition method. *Proceedings of the Royal Society of London, 460A*, 1597–1611.

Wu, Z. H., & Huang, N. E. (2009). Ensemble empirical mode decomposition: A noise assisted data analysis method. *Advances in Adaptive Data Analysis, 1*, 1–41.

Wu, J. D., & Liu, C. H. (2008). Investigation of engine fault diagnosis using discrete wavelet transform and neural network. *Expert Systems with Applications, 35*(3), 1200–1213.

Zarei, J., & Poshtan, J. (2009). An advanced Park's vectors approach for bearing fault detection. *Tribology International, 42*, 213–219.

Zhang, Q. H., & Benveniste, A. (1992). Wavelet networks. *IEEE Transactions on Neural Networks, 3*, 889–898.